THE IMPACT OF BOUNDARY LAYER SEPARATION CONTROL ON A PLANE MIXING LAYER

R. Mathis, E. Collin, J. Delville, and J.P. Bonnet
Laboratoire d'Etudes Aérodynamiques,
UMR CNRS 6609 - Université de Poitiers - ENSMA
C.E.A.T., 43, route de l'Aérodrome F-86036 Poitiers - France
romain.mathis@lea.univ-poitiers.fr

ABSTRACT

The purpose of this experimental study is to analyze the effects of a driven separation near the trailing edge of a splitter-plate on the development of a turbulent mixing layer. The separation is driven by a steady pneumatic injection, and is considered here as an actuator for controlling the mixing efficiency of the mixing layer. Particle image velocimetry and hot wire measurements are performed for the natural and the manipulated regimes. The results highlight the hyper-mixing capabilities of the control strategy. Analyses of the turbulent field and coherent structures organization give essential information about the mechanisms responsible for the mixing enhancement.

INTRODUCTION

As reviewed widely by Fielder (1998) and Gutmark et al. (1995), shear layer control is a key topic for many industrial applications. This study deals with a new mixing enhancement technique. The patented concept is based on a flow regime close to boundary layer separation on a beveled splitter plate (Fig. 1). The flow is naturally attached on the bevel. A perturbation is imposed upstream of the bevel which induces a separation of the flow over it. The separation itself can be controlled by many ways, e.g. by using a corona effect (Labergue et al., 2004) or by using a pneumatic injection normal to the wall (Mathis et al. 2004). This latter device is used in the present study. Previous studies have shown that this strategy leads to a consistent mixing enhancement (Mathis et al. 2004). This actuator generates a recirculation bubble near the splitter plate trailing edge, which increases the turbulent activity and the three dimensionality of the flow. This perturbation, as appearing at the location of maximum receptivity of the mixing layer, has a large effect on the downstream evolution of the flow. Thus, the mixing layer spreading rate is found to be doubled in the manipulated regime, even far downstream of the splitter plate. The aim of the present study is to explore the turbulent balance and coherent structures organization in this manipulated mixing layer, for a better understanding of the way the mixing enhancement is achieved. We focus here on an area downstream of the trailing edge that extends over less than 4 times the bevel length.

EXPERIMENTAL SETUP

The experiments are carried out in a subsonic closed loop wind tunnel on a plane air/air mixing layer. The settling chamber is divided by a plate into two parts, of different head losses in order to generate two different velocities. Sand paper is glued on each side of the splitter-plate in order to generate fully turbulent boundary layers. The test section is squared 300×300 mm^2 and 2 m long. The plane mixing layer has a velocity ratio $r = U_2/U_1 = 0.66$, with a high-velocity $U_1 = 33$ m/s. The low-velocity is $U_2 = 22$ m/s. The boundary layers thicknesses δ_{99} upstream of the bevel are 6.75 mm ($H = 1.49$) and 6.45 mm ($H = 1.43$) for the high- and low-speed sides, respectively. The velocity difference, $\Delta U = U_1 - U_2$, is used

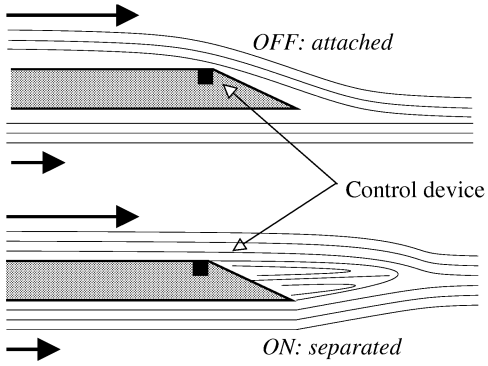

Figure 1: Control concept.

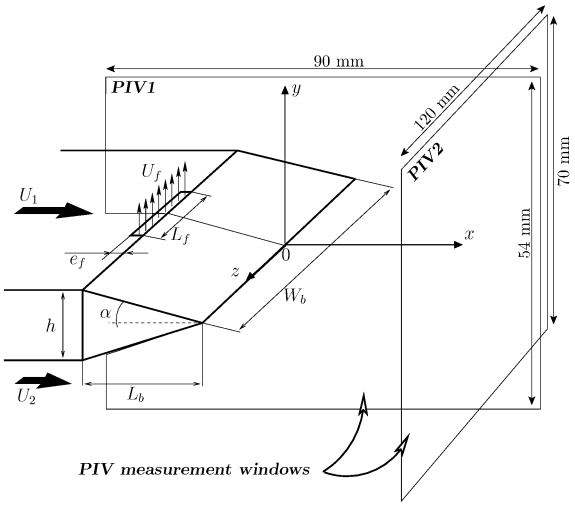

Figure 2: Experimental setup.

for data normalization: $u^* = (u - U_2)/\Delta U$. The splitter-plate is thick, $h = 19$ mm, and its trailing edge is beveled with a half angle $\alpha = 12^o$, so that the flow is naturally attached but close to separation. The Reynolds number based on the shear velocity ΔU and the thickness of the splitter-plate h is $Re = 13,700$.

The separation is driven on the high-speed side of the bevel, by a forcing steady jet blowing at the velocity U_f through a rectangular slot ($L_f \times e_f = 40 \times 0.7$ mm^2) located at the beginning of the bevel (Fig. 2). The velocity ratio between the forcing jet and the high-speed free stream is $U_f/U_1 = 0.75$. Direct axis (x, y, z) are used, where the origin is located at the trailing edge in the median plane of the slot, corresponding to the velocity components (u, v, w).

The measurements are performed by several means:

- Hot-wire and Pitot-static pressure measurements are used in a preliminary study.
- Particle Image Velocimetry (PIV) measurements are performed with a *LAVISION* system with a Nd-YAG laser (30 mJ) and 12 bits CCD cameras. The seeding is obtained from pulverised olive oil particles. Two arrangements are used. Firstly, a 2-components PIV (PIV1) is performed in the $(x, y, z = 0)$ plane (Fig. 2) that aims at analysing the flow characteristics near the bevel, where 450 instantaneous (u, v) velocity fields are collected. Secondly, a stereo PIV (PIV2) is performed in (y, z) planes located at various downstream locations ($x/L_b = 0.1$, 1, 2, 3 & 4) (Fig. 2). For this experiment, 1000 instantaneous (u, v, w) velocity fields are collected. The sample size retained for each PIV experiment has been chosen to ensure convergence of the statistics for the average velocity, longitudinal vorticity and Reynolds stresses.

RESULTS

Natural mixing layer

The mixing layer in the natural case has a self similar behaviour starting at $x/L_b = 9$ (see Fig. 3). From this point, the mixing layer develops in the same way as a classical mixing layer. Its spreading rate is close to the one observed by many authors (e.g. Pope, 2000). The initial region corresponds to a wake effect, reinforced by the non parallel character of the flows arising at the trailing edge. The Reynolds stresses distribution and levels are found in agreement with conventional results.

Mean velocity field

A local characteristic thickness of the mixing layer $b(x, z)$ is defined corresponding to $y_{0.9} - y_{0.1}$, where $y_{0.9}$ and $y_{0.1}$ correspond to $\overline{u}^*(y_{0.9}) = 0.9$ and $\overline{u}^*(y_{0.1}) = 0.1$, respectively. An average spreading rate $d\overline{b}(x)/dx$ of the controlled mixing layer can be defined, where $\overline{b}(x) = \int_{-L_z/2}^{-L_z/2} b(x, z)dz$ and where L_z is the spanwise extend on which the perturbation is observable (see Fig. 5). The longitudinal distribution of $\overline{b}(x)$ is plotted compared to the natural case in Fig. 3. A very large increase of the spreading rate is created by the separation (about 2 times the natural one). It is also observed that the mixing layer develops linearly earlier than the natural case: the linear development starts at $x/L_b = 2$ in the manipulated case.

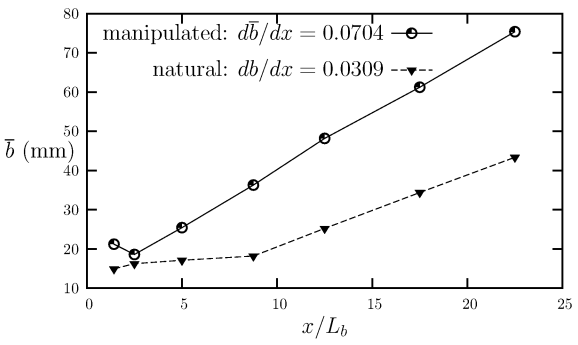

Figure 3: Streamwise evolution of the spreading rate $d\overline{b}/dx$ (Pitot tube measurements).

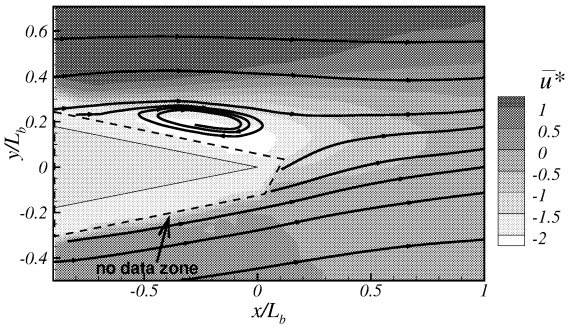

Figure 4: Mean streamwise velocity $\overline{u}^*$ and streamlines in the vicinity of the boundary layer separation, ($z = 0$) plane (PIV1).

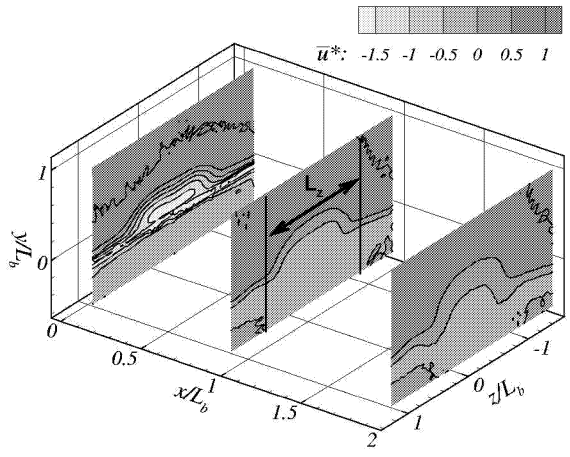

Figure 5: Mean streamwise velocity $\overline{u}^*$ downstream of the boundary layer separation (PIV2).

The mean streamwise velocity field obtained very close to the trailing edge from the PIV1 measurements is shown in Fig. 4. The boundary layer separation, characterized by a recirculation bubble, appears clearly on the bevel. This effect can also be retrieved on the surface flow visualisation by traces

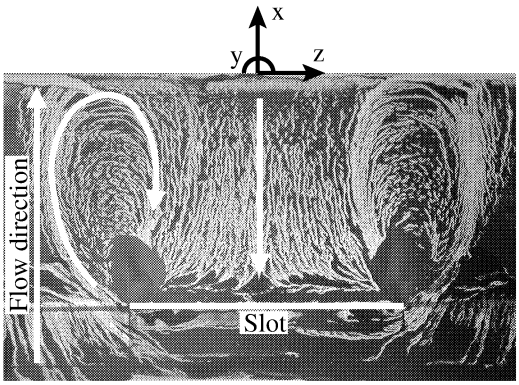

Figure 6: Surface flow visualisation on the bevel.

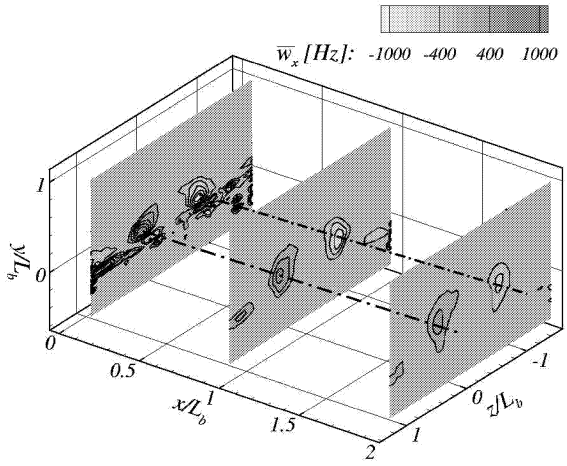

Figure 7: Streamwise vorticity, $\overline{\omega}_x$ downstream of the boundary layer separation (PIV2).

going upstream for $z = 0$ (Fig. 6). The separation is followed by a strong wake effect visible in Fig. 4 and 5 as illustrated by negative values of $\overline{u}^*$. Downstream of the trailing edge, streamlines are deflected toward the high velocity side. Indeed, it is remarkable that the maximum velocity deflect of the downstream velocity profile $\overline{u}^*(y)$ is found to be centered at $y/L_b = 0.15$, i.e. right downstream of the recirculation bubble. Moreover, the mean streamwise velocity field obtained by the PIV2 measurements shows a three-dimensional deformation of the $\overline{u}^*$-velocity field (Fig. 5). This could indicate that the mixing enhancement is mainly generated by three-dimensional mechanisms. For this reason, the study is focused on the near region of the trailing edge where the phenomena responsible of the mixing seem to occur.

The corresponding mean streamwise vorticity data obtained by PIV2 is shown in Fig. 7. A strong streamwise vorticity concentration is produced on both sides of the separation region at $z/L_b = \pm 0.5$, where a pair of counter rotating vortices clearly appear. The two structures develop in parallel downstream with a small shift toward the high-speed side of the mixing layer. These vortices are probably due to the fact that the separation is limited in the spanwise direction. Indeed, Fig. 6 shows a surface visualisation on the bevel, where two counter-rotating structures appear on both sides of the boundary layer separation. Furthermore, the closed traces pattern leads us to think that a vertical vorticity ω_y coexists with the streamwise vorticity ω_x.

These 3D aspects are close to those obtained by "delta-tabs". Indeed, Foss and Zaman (1999) have shown similar effects with a "delta-tabs" placed on the high-speed side on the trailing edge. However, in their case no wake appears, whereas in our case the wake is generated by the separation over the bevel: there is a complex interaction between the wake and the streamwise vorticity induced by the boundary layer separation. On the other hand, the boundary layer separation is quite efficient as it produces hyper-mixing ($\overline{b} \times 2$), which has not been observed in precedent studies for pneumatic mixing enhancement devices (see for example the work of Collin et al., 2004). In other words, we take benefit of the amplification effect due to the flow configuration which is at the verge of the separation.

Reynolds stresses

Reynolds stress fields obtained by PIV and normalized by ΔU^2 have been studied. Each component is strongly increased compared to the level obtained in the natural mixing layer. For example, the turbulent kinetic energy k and the Reynolds shear stress $\overline{u'v'}$ are plotted in Fig. 8 and 9, respectively. The higher levels observed at the first measurement location ($x/L_b = 0.1$) are more than 15 times stronger than those in the natural case. The Reynolds stresses decrease with the downstream location, without any significant spanwise diffusion. Fig. 10 shows the streamwise evolution of the maximum value of k and the minimum value of $\overline{u'v'}$ obtained in the median plane z/L_b=0. The strong difference of level appears clearly near the trailing edge between the natural (dashed line) and the manipulated case (solid line). Downstream the diffusion of k_{max} and $\overline{u'v'}_{min}$ is observed, corresponding to an exponential decrease towards the natural state.

On the (x, y) plane representation of the $\overline{u'v'}$, shown in Fig. 11, a maximum localised just downstream of the boundary layer separation is observed, in the wake region (cf Fig. 4). The same result is found on the turbulent kinetic energy k, which leads to interpret that the high level of the Reynolds stress components are responsible for the hyper-mixing observed in Fig. 3. On the other hand, this could indicate that the production of turbulent shear stress is generated by an unsteady behaviour downstream of the separation, and not only by the wake itself. An overview of the coherent structures in this region of the flow is given in the next section.

For a better understanding of the phenomena, a comparison between the $\overline{u'v'}$ and the $\partial\overline{u}/\partial y$ profiles in the wake region ($x/L_b = 0.1$) is given in Fig. 12. Although the $\partial\overline{u}/\partial y$ profile is clearly asymmetrical, the $\overline{u'v'}$ profile is strongly unbalanced. Strong values of the turbulent shear stress are found only in the high-speed part of the wake-shear layer. The differences between the $\overline{u'v'}$ and the $\partial\overline{u}/\partial y$ profiles make Boussinesq closure model incompatible with this flow configuration. The profiles given in Fig. 12 also show that the production term ($\overline{u'v'}\ \partial\overline{u}/\partial y$) is strongly unbalanced too. Turbulent production occurs mainly downstream the boundary layer separation, i.e. only in the high-speed side of the wake-shear layer. It should be noted that the negative values of $\partial\overline{u}/\partial y$ are also partly due to the local change in the flow direction (see streamlines in Fig. 11), which does not produce turbulence.

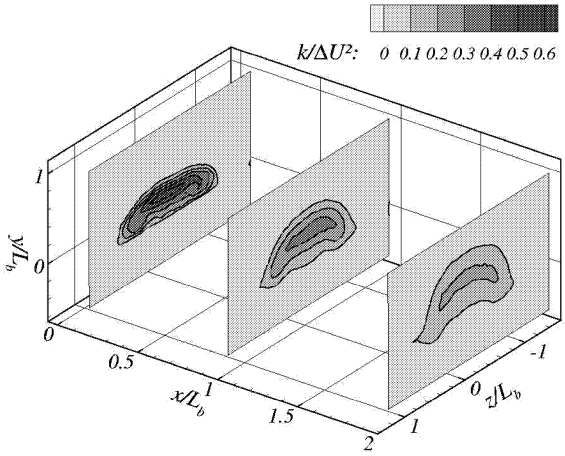

Figure 8: Turbulent kinetic energy $k/\Delta U^2$ downstream of the boundary layer separation (PIV2).

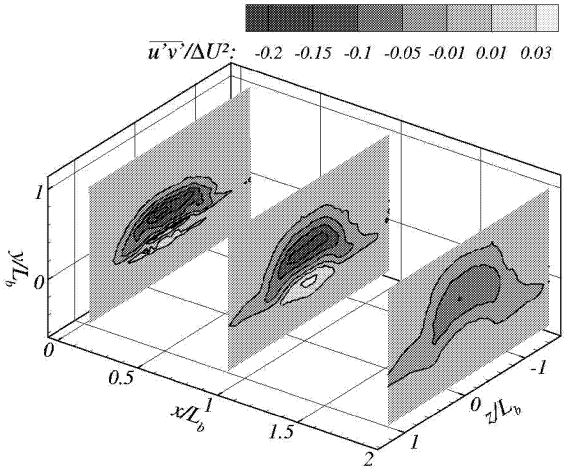

Figure 9: Cross-component $\overline{u'v'}/\Delta U^2$ downstream of the boundary layer separation (PIV2).

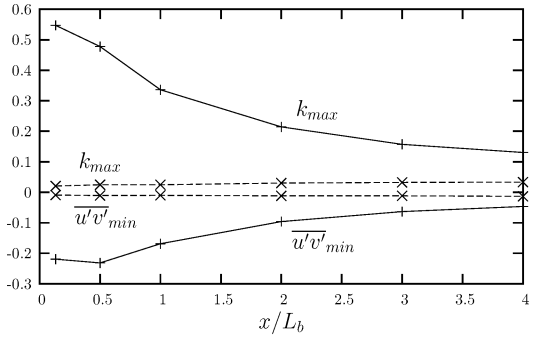

Figure 10: Streamwise evolution of the $k_{max}/\Delta U^2$ and $\overline{u'v'}_{min}/\Delta U^2$ for the $k(y)$-profile and $\overline{u'v'}(y)$-profile in the median plane $z/L_b = 0$ (-×- is the reference of the uncontrolled data) (PIV2).

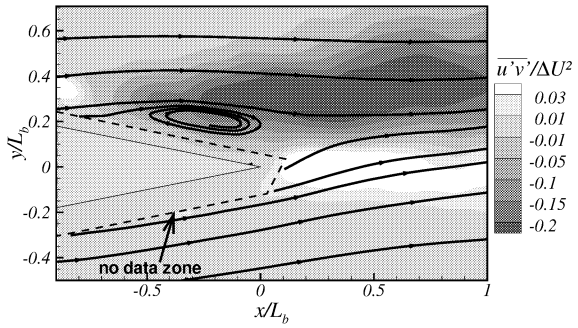

Figure 11: Cross-component $\overline{u'v'}/\Delta U^2$ and streamlines in the vicinity of the boundary layer separation (PIV1).

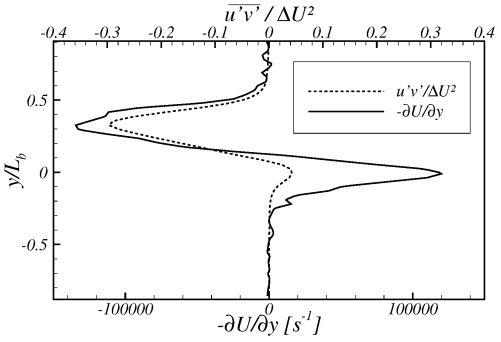

Figure 12: Profile of $\overline{u'v'}$ and $-\partial\overline{u}/\partial y$ in the middle plane of the mixing layer, in the wake region ($x/L_b = 0.1$, $z/L_b = 0$) (PIV1).

The other components of the Reynolds stress tensor depict the complex 3D effects occurring in the mixing layer. Among these components, a production of $\overline{u'w'}$ and $\overline{v'w'}$ is noticed (Fig. 13 and 14), which is characteristic of the three-dimensional organization of the flow induced by the vortices structures. In fact, the flow is an interaction of two wakes: a "vertical wake" ($\partial\overline{u}/\partial y < 0$) similar to the one created by an horizontal blunt trailing edge, and a "spanwise wake" ($\partial\overline{u}/\partial z \neq 0$) similar to the one created by a vertical bluff body introduced in free stream flow. Furthermore both wakes are coupled with the mixing layer which develops downstream. Then, the $\overline{u'w'}$ production is mainly induced by the "spanwise wake", whereas the $\overline{v'w'}$ is mainly induced by the "vertical wake". It is also noticed that the minimum and maximum location of $\overline{u'w'}$ are right downstream both sides of the separation region on the bevel which is characterized by a $\partial u/\partial z = 0$ on the traces (Fig. 6).

Flow organization

A Proper Orthogonal Decomposition (POD) (Lumley, 1967, Sirovich, 1987) has been performed on the PIV1 fields. A *snapshot*-POD is used (Sirovich, 1987) to filter the (u, v)-velocity field: a partial reconstruction of these fields is performed to take into account the modes #1 to 17 which represent 75% of the velocity field energy (among the 450 POD modes necessary to obtain 100% energy). This has been performed on 6 velocity field samples. Fig. 15 shows such reconstructions. Firstly, the separation does not consist of a steady recirculation bubble. Secondly, it is observed that the

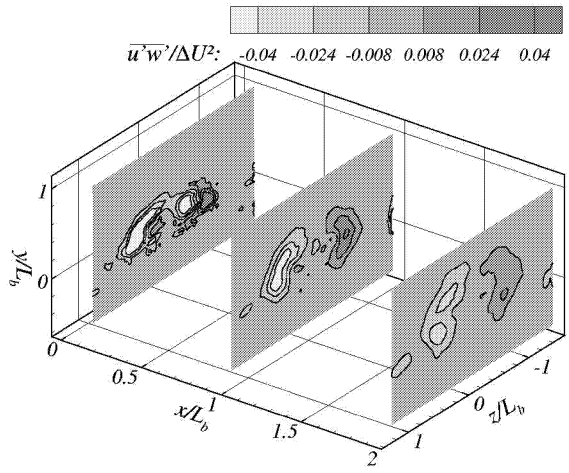

Figure 13: Cross-component $\overline{u'w'}/\Delta U^2$ downstream of the boundary layer separation (PIV2).

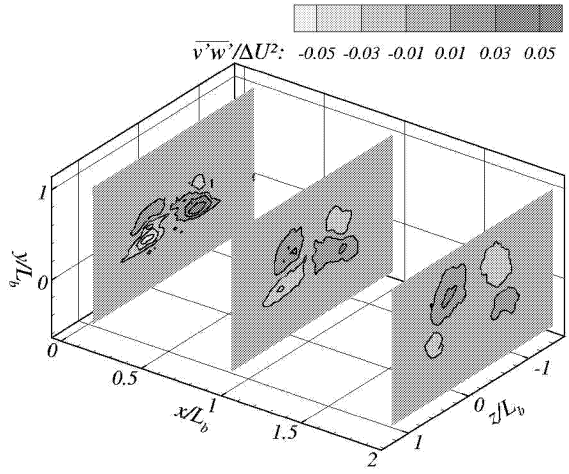

Figure 14: Cross-component $\overline{v'w'}/\Delta U^2$ downstream of the boundary layer separation (PIV2).

large scale structures are produced in the wake region. These structures interact with the mixing layer just downstream of the separation. This may be linked to the strong Reynolds stresses production in this region of the flow.

Furthermore, a movement at the trailing edge of the low-speed flow toward the separation bubble is observed on some (u, v)-velocity fields. This results confirms the flow communication between the two sides of the trailing edge that has been already observed in preliminary studies (cotton tufts glued on the low-speed side of the trailing edge).

A spectral analysis of the fluctuating longitudinal velocity highlights the differences between the natural case and the manipulated regime. The Fig. 16 shows spectra obtained with a single hot wire probe located in the $(z/L_b = 0)$-plane at $x/L_b = 1.1$ for a y-locations near the low-speed side boundary of the mixing layer $(\overline{u}^*(y) = 0.25)$. In the manipulated regime, an increase of energy appears for a wide bandwidth at low frequency $(St = fh/U_1 < 0.4)$, whereas the inertia range of the spectra does not seem to be significantly affected by the control. The bandwidth for which the energy increases is centered on a frequency which corresponds to $St = 0.2$. This frequency is characteristic of a blunt trailing edge instability (Perret et al., 2003). However, the very large-scale structures shown in Fig. 15 are not characterized by a sharp peak at $St = 0.2$. This feature may be due to strong three-dimensional effects in the manipulated case. The spectral behaviour confirms the unsteady character of the separation, although the control of the separation itself is steady.

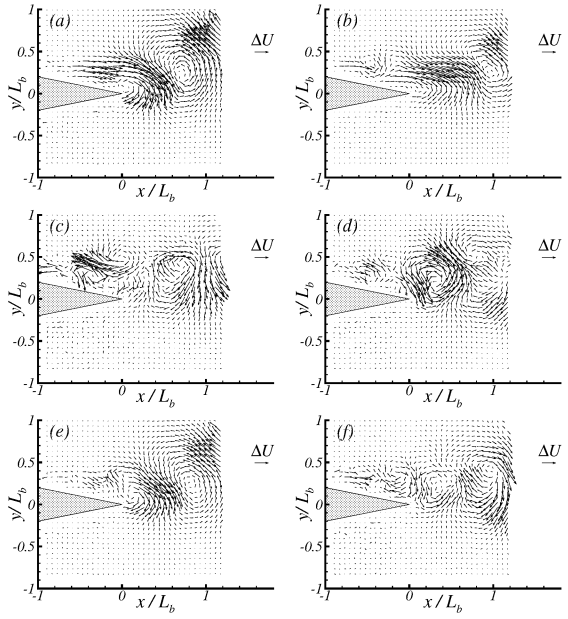

Figure 15: Examples of instantaneous unsteady velocity field, POD-filtered data with 75% of the velocity field energy (PIV2).

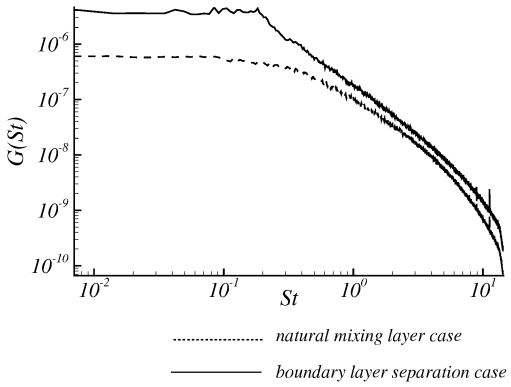

Figure 16: Energy spectral density at the location $(z = 0, x/Lb = 1.1)$ where $\overline{u}^*(y) = 0.25$ (hot-wire).

CONCLUSION

The influence of a separation over a bevel on a mixing layer was studied experimentally. The main features occurring downstream of the boundary layer separation have been studied using Particle Image Velocimetry, Pitot-tube and hot-wire.

A statistical approach allows us to describe the three-dimensional aspects of the manipulated mixing layer. These effects are the result of an interaction between two wakes and a mixing layer, which induces a hyper-mixing. It is clear that the localised controlled separation induces longitudinal vorticity that enhance mixing. These results suggest that this unsteadiness is a key process that can contribute to energize large scale structures in the mixing layer, promoting hyper-mixing. We show that the use of a steady blowing allows strong unsteady 3D perturbations of the initial conditions of the turbulent mixing layer with dramatic influence on the downstream mixing. These results are obtained in taking benefit of the natural time and energy amplification of a flow close to the separation. Proper scaling in size and frequency can be defined according the expected more amplified modes of the mixing layer to be controlled. This will be applied on an axi-symmetric jet to excite the unsteady modes in order to enhance the mixing.

ACKNOWLEDGMENTS

Support of this work was provided by the CNRS, Region Poitou-Charentes and the French Ministry of Research through the COS program. The authors also thank Carine Fourment and Patrick Braud for their assistance in measurements.

REFERENCES

Collin, E., Barre, S., and Bonnet, J.P., 2004, "Experimental study of a supersonic jet-mixing layer interaction", *Physics of Fluids*, vol. 16, issue 3, pp. 765-778.

Fielder, H.E., 1998, "Control of free turbulent shear flows", *Flow Control "Fundamentals and Practice"*, of Bonnet J.P., Gad-el Hak M., Pollard A., pp. 335-429.

Foss, J.K., and Zaman, K.B.M.Q., 1999, "Large- and small-scale vortical motions in a shear layer perturbed by tabs",*Journal of Fluid Mechanics*, vol.382, pp. 307-329.

Gutmark, E.J., Schadow, K.C, and Yu, K.H, 1995, "Mixing enhancement in supersonic free shear flows", *Annual Review of Fluid Mechanic*, vol. 27, pp. 375-417.

Labergue, A., Léger, L., Moreau, E., Touchard, G., and Bonnet, J.P., 2004, "Experimental study of the detachment and the reattachment of an airflow along an inclined wall by a surface corona discharge - Application to a plane turbulent mixing layer", *IEEE Transactions on Industry Applications*, Vol. 40, No. 5, pp. 1205-1214.

Lumley, J.L., 1967,"The Structure of Inhomogeneous Turbulent Flows", *Atm. Turb. and Radio Wave Prop.. Yaglom and Tatarsky eds. Nauka, Moscow*, pp. 166-178.

Mathis, R., Collin, E., Delville, J., and Lebedev, A., 2004, "On the dynamics of the transition between attached and separated conditions at mixing layer origin", *Proceedings of the 10th European Turbulence Conference, Trondheim, Norway*, pp. 721-724.

Perret, L., Delville, J. , and Bonnet, J.P., 2003, "Investigation of the large scale structures in the turbulent mixing layer downstream a thick plate", *Proceedings of the 3rd International Symposium on Turbulence and Shear Flow Phenomena, Sendai, Japan.*

Pope, S.B., 2000, "Turbulent Flows", Cambridge, University Press.

Sirovich, L., 1987, "Turbulence and the Dynamics of Coherent Structures, Part 1: Coherent Structures",*Quarterly of Applied Mathematics, XLV, 3 561-571*